Quantum Hall effect on centimeter scale chemical vapor deposited graphene films

Tian Shen,[1,2,∗] Wei Wu,[3] Qingkai Yu,[3] Curt A Richter,[2]

Randolph Elmquist,[2] David Newell,[2] and Yong P. Chen[1,4,5]

[1]*Department of Physics, Purdue University, West Lafayette, IN, 47907*

[2]*Physical Measurement Laboratory, National Institute*

of Standards and Technology, Gaithersburg, MD, 20899

[3]*Center for Advanced Materials and ECE,*

University of Houston, Houston, TX, 77204

[4]*Birck Nanotechnology Center, Purdue University, West Lafayette, IN 47907*

[5]*School of Electrical and Computer Engineering,*

Purdue University, West Lafayette, IN 47907

(Dated: October 3, 2011)

Abstract

We report observations of well developed half integer quantum Hall effect (QHE) on mono layer graphene films of 7 mm × 7 mm in size. The graphene films are grown by chemical vapor deposition (CVD) on copper, then transferred to SiO_2/Si substrates, with typical carrier mobilities ≈4000 cm^2/Vs. The large size graphene with excellent quality and electronic homogeneity demonstrated in this work is promising for graphene-based quantum Hall resistance standards, and can also facilitate a wide range of experiments on quantum Hall physics of graphene and practical applications exploiting the exceptional properties of graphene.

∗Electronic address: tshen@nist.gov

Graphene, a single sheet of carbon atoms tightly packed into a two-dimensional (2D) hexagonal lattice, has been considered as a promising candidate for the next generation high-speed electronic devices due to its extraordinary electronic properties, such as a carrier mobility exceeding 10 000 cm^2/Vs and an electron velocity of $\approx 10^8$ cm/s at room temperature.[1] Monolayer graphene's massless fermion nature gives rise to a characteristic "half-integer" quantum Hall effect (QHE). The associated Landau level (LL) separation, $\Delta(E) = (\sqrt{n+1} - \sqrt{n})v_F\sqrt{2eB\hbar}$, is anomalously large for even moderate magnetic fields.[2, 3] For example, at a magnetic field of 10 T, the LL gap between the n=0 and n=$\pm$1 LL is $\approx$1300 K in graphene compared to $\approx$200 K in GaAs heterostructures, enabling the observation of QHE at high temperatures,[4] and raising exciting possibilities for future quantum Hall resistance metrology based on graphene.[5, 6] Graphene flakes, typically only a few microns in size, as produced by mechanical exfoliation onto SiO$_2$ [7] are considered to be too small for resistance metrology applications. The recent demonstration of half-integer quantum Hall effect in monolayer graphene epitaxially grown on both Si face[6, 8, 9] and C face[10] of SiC, and grown by chemical vapor deposition (CVD) on Ni[11] and Cu[12, 13], suggests that graphene produced by such more scalable approaches can have advantages for metrology applications. However, due to charge inhomogeneity[14], QHE has so far only been observed in samples of size up to $\approx$100 μm$\times$100 μm. In this letter, we demonstrate CVD graphene grown on Cu with size approaching centimeter scale possessing excellent electronic properties as evidenced by well-developed half-integer QHE. Our results are important not only for the development of graphene based quantum Hall resistance standards, but also for other practical applications of graphene that desire large scale samples with excellent electronic quality and uniformity, such as integrated circuits and transparent conducting electrodes.[11] Such high-quality and large-scale graphene films will also facilitate a wide range of experiments, such as optical studies and scanning tunneling microscope (STM) studies of graphene's QHE and other electronic properties.

The graphene samples studied here are synthesized by CVD of CH$_4$ on Cu foils (25 μm thick, 99.8 %) in a quartz tube furnace at ambient pressure.[12, 15] Before graphene deposition, Cu foils are annealed in Ar and H$_2$ at 1050 °C for 30 min to clean the Cu surface and increase the Cu grain size. Graphene growth is then carried out under 15 parts-per-million (ppm) CH$_4$ (balanced in Ar and H$_2$) at 1050 °C for 25 min. To transfer graphene to SiO$_2$/Si substrates, the as-synthesized samples are spin-coated by polymethyl methacrylate
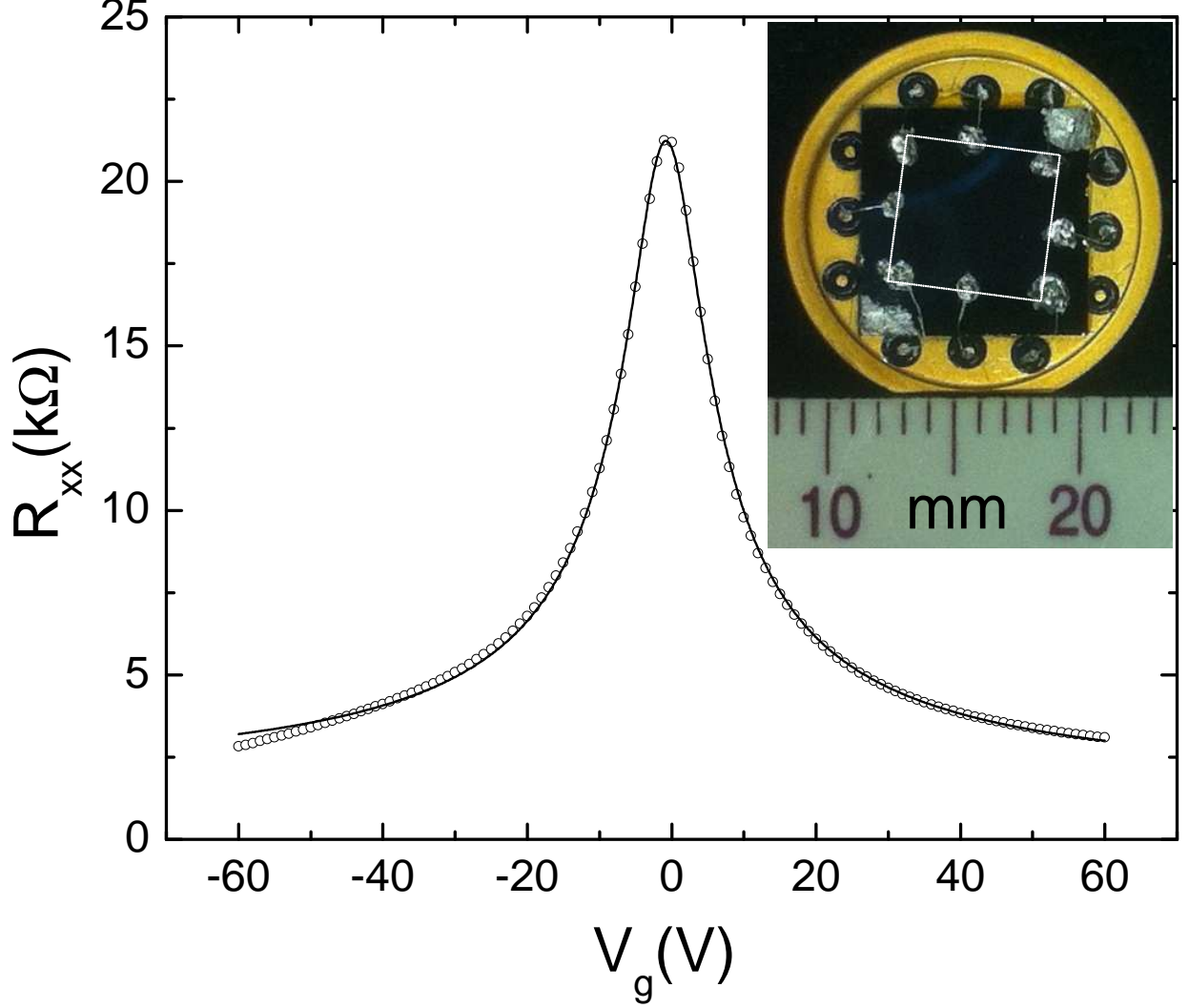
Figure 1: DC four-terminal longitudinal resistance R_{xx} (hollow circle) measured as a function of gate voltage V_g at 1.7 K along with modeling fit (solid line). Insert: Picture of the 7 mm×7 mm graphene device on a SiO_2/Si substrate. The dashed square is a guide to the eye indicating the outline of the graphene film.

(PMMA) and placed in an aqueous solution of iron nitrate to etch away the Cu substrate. Afterwards, the graphene with PMMA coating is scooped out from the solution directly onto the transfer substrate. After carefully rinsing in acetone and isopropanol to remove the PMMA residues induced in the transfer process, indium contacts both to graphene and backside silicon are made to form a Van der Pauw device, as shown in Fig. 1 insert. The sample is then immediately cooled down in a variable temperature [4]He cryostat (1.6 K to 300 K) to minimize the exposure to atmosphere, which introduce hole doping and

increase disorder in the graphene films.[16] Four-point magneto-transport measurements are performed in magnetic fields up to 14 T using both the low frequency ac lock-in technique and current reversed dc technique with a source-drain (SD) input current of 100 nA for fast or precise characterizing of the device performance. We perform the dc resistance measurements using a dc current source and three $8^1/_2$ digit multimeters, two for V_{xx}, V_{xy} and one for V_{cal}, measured across a 10 kΩ resistance standard (in series of the sample) whose value is known better than 1 ppm. The measured values of V_{cal} are used for cross-checking the current and calculating of R_{xx} and R_{xy}. The carrier density is tuned by a back gate voltage V_g applied between the highly doped Si substrate and the graphene, with the 300 nm SiO$_2$ as the gate dielectric. Measurements on two such devices yield similar results, however data for only one of them are presented below.

Figure 1 shows the dc four terminal longitudinal resistance R_{xx}, configured as in Fig. 2 (c), measured at 1.7 K and zero magnetic field with V_g from -60 V to 60 V. It shows ambipolar field effect with resistance modulation ratio greater than seven. The Dirac point, V_{Dirac}, in the device is situated at -0.7 V, indicating a very low extrinsic charge doping level. This is expected since no fabrication is performed on this device, and the contamination introduced during common fabrication processes is minimized. In our sample, the accuracy of the simple Van der Pauw method to extract the resistivity (thus the mobility) may be limited due to rough edges, large contact sizes and voids inside the film that change the current path. Therefore, we have used a self-consistent approach to fit the field effect curve (see [29]), and extracted both a geometrical factor of 4.2 ± 0.7 and a field effect mobility of (3600 ± 600) cm^2/Vs. A Hall mobility of (4000 ± 700) cm^2/Vs at V_g= -30 V is obtained by applying the same geometrical factor, consistent with the field effect mobility.

To further characterize the film quality and characteristic quantum Hall effect, we have measured R_{xx} and R_{xy} versus B (perpendicular magnetic field) at fixed $V_g = -9$ V as shown in Fig. 2 (b). The $i = \pm2$ quantum Hall plateaus are well resolved. The higher LL plateaus are still not visible, due to disorder induced LL broadening. Below we focus on measurements by sweeping V_g at the highest available magnetic field, where better quality quantum Hall states are observed. The dc measurements are carried out in both four-terminal and two-terminal configuration as a function of V_g at 1.7 K with $B = 14$ T as shown in Fig. 2 (a). The resistances are (anti)symmetrized between positive and negative magnetic field orientations to compensate for the imperfect geometry. The longitudinal
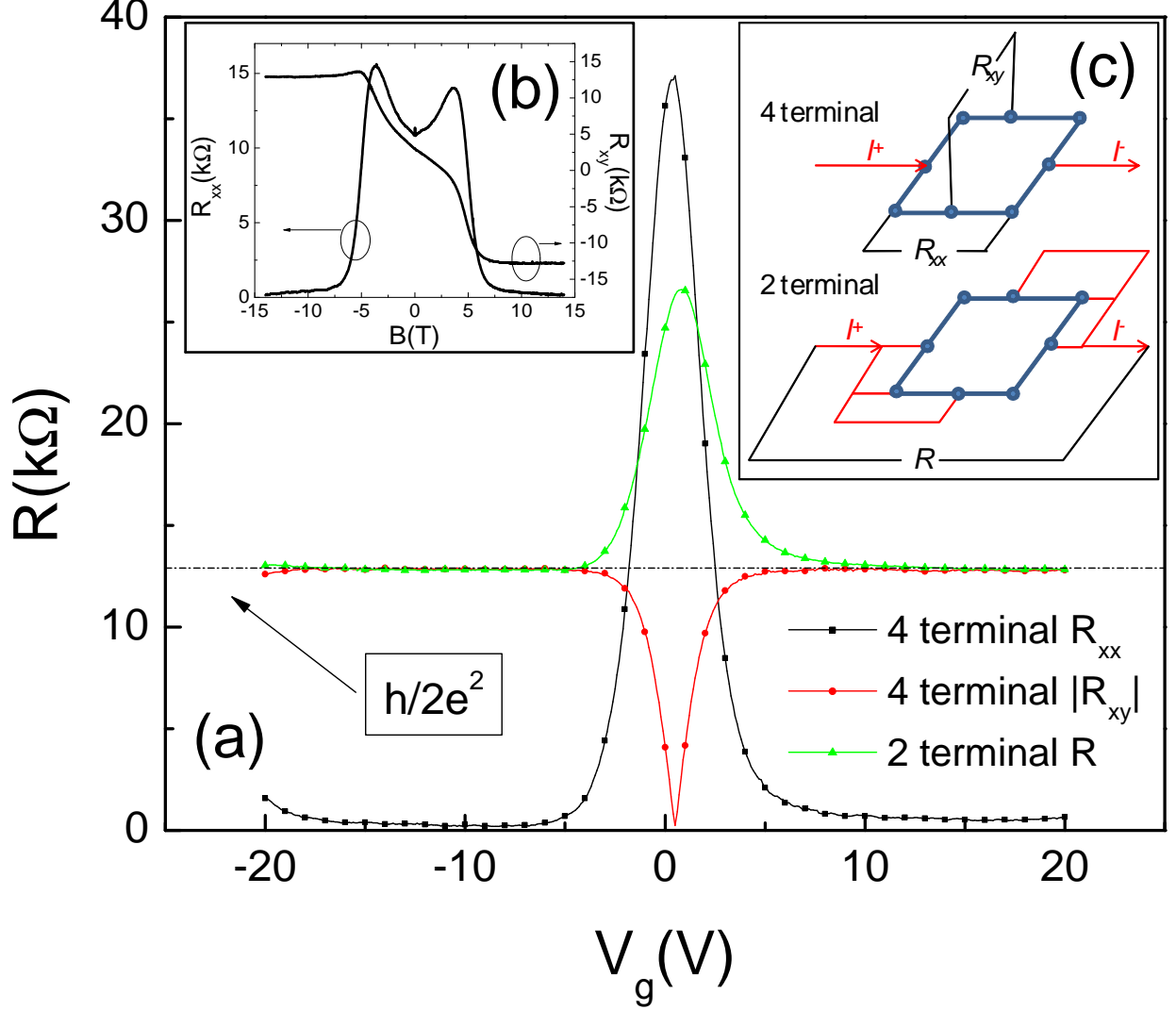
Figure 2: (a) DC four-terminal longitudinal resistance R_{xx}, absolute value of Hall resistance $|R_{xy}|$ and two-terminal resistance R as a function of V_g measured at 1.7 K and a magnetic field of 14 T. The resistances are (anti)symmetrized between positive and negative magnetic fields. The horizontal dashed line is the $h/2e^2$ conventional value as assigned in 1990.[17] (b) R_{xx} and R_{xy} as a function of magnetic field at 1.7 K and V_g=-9 V. (c) Schematic circuit diagram for four terminal and two terminal triple-series measurements. The solid dots represent the indium contacts as shown in Fig. 1 insert.

resistance R_{xx} shows low minimum values indicating quantum Hall states in the ranges of -18 V to -5 V for holes and 10 V to 20 V for electrons. The Hall resistance R_{xy} shows well developed quantum Hall plateaus at the corresponding R_{xx} minima. The sharp $i = 2$ to

$i = -2$ quantum Hall plateau to plateau transition happens within a gate voltage range of (1.5 ± 0.4) V (measured between two extrema in the derivative $d\sigma_{xx}/dV_g$ for $n = 0$ LL), comparable with the transition for exfoliated graphene.[18] This also confirms that the inhomogeneity in our large graphene film is small, as large inhomogeneity will tend to broaden the transition and even destroy the quantum Hall effect. The observed quantum Hall resistances are not exact, showing a residual R_{xx} of $\approx 200\ \Omega$ for holes ($i = -2$ state) and $\approx 500\ \Omega$ ($i = +2$ state) for electrons. R_{xy} also deviates from $h/2e^2$ (the dashed horizontal line) by $\approx 50\ \Omega$ for holes and $\approx 100\ \Omega$ for electrons, qualitatively consistent with the theory that the absolute error in the quantization of ρ_{xy} ($=R_{xy}$) can be related to a finite resistivity ρ_{xx} (indicating dissipation) as $\Delta\rho_{xy} = -s\rho_{xx}$, where s is on the order of unity.[19] While the four-terminal resistance measurement is widely used to eliminate the effect of contacts and wires, two terminal triple-series connections proposed by Delahaye [20, 21] can also be used in both dc and ac bridges for high precision measurements of QHE. Assuming all of the contact and wire resistance values $R_c, R_w \ll R_H = h/2e^2$, then from the dc equivalent circuit model, [22] the resulting two-terminal resistance for a perfectly quantized $i = \pm 2$ plateau is:

$$R = R_H \left(1 + 2 \left(\frac{R_c + R_w}{R_H} \right)^3 \right). \tag{1}$$

Considering a few ohms of resistance presented in the wire, then $R_c < 10\ \Omega$ is generally desired to achieve the precision of a few parts per billion when using R to measure the QHE. This is an experimental challenge for micron-sized graphene devices since the best normalized contact resistance so far is still $\approx 500\ \Omega\mu$m.[23] Large contact resistance also introduces noise on the voltage probes, and leads to local heating at the current contacts thereby limiting the maximum breakdown current of QHE. The scalability of CVD graphene makes it possible to use large area contacts to reduce contact resistances. In our device, the contact size is $\approx$1 mm, thus R_c can easily fall below 10 Ω assuming a reasonable normalized contact resistance, i.e. ≈ 5 k$\Omega\mu$m for indium and clean graphene surface. While the precise determination of the contact resistance from our measured QHE plateau is difficult due to a non-vanishing R_{xx}, the measured two terminal R agrees well with four terminal R_{xy} at the center of plateau, indicating that the contact resistance is likely much smaller than the residual R_{xx} and does not play a significant role here.

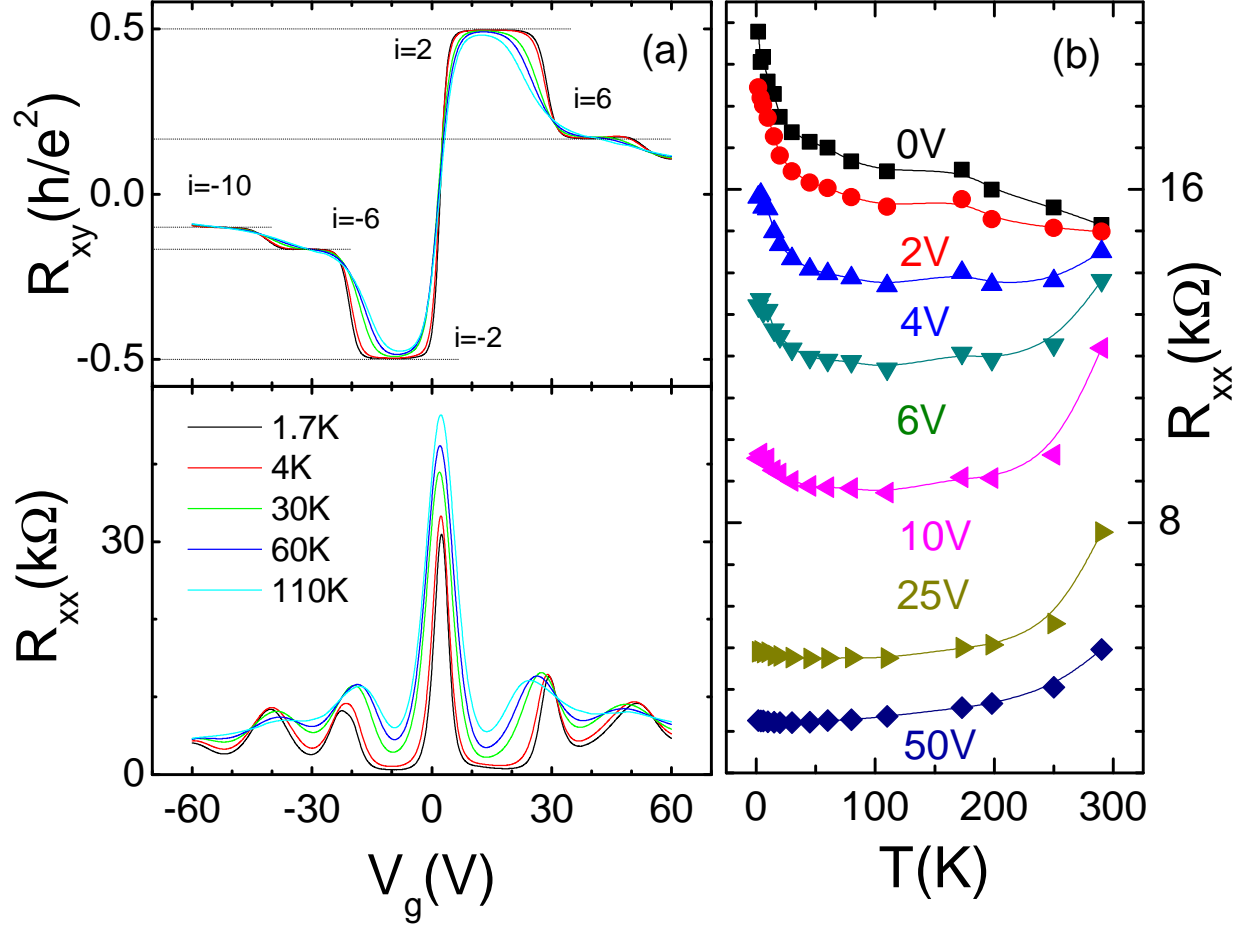To investigate the reliability of this device, the sample is warmed up and exposed to

Figure 3: (a) Hall resistance R_{xy} and longitudinal resistance R_{xx} as a function of V_g at B=14 T for different temperatures. The resistances are (anti)symmetrized between the positive and negative magnetic field orientations. The horizontal dotted lines indicate the $i = \pm 2$, ± 6 and -10 quantum Hall plateau conventional values as assigned in 1990.[17] (b) $R_{xx}(T)$ at various ΔV_g at B=0 T. The symbols are experimental data and the lines are guides to the eye.

atmosphere for 24 h and then cooled back down again. An ac lock-in technique is used for fast characterization. R_{xx} and R_{xy} are measured as a function of V_g at B=$\pm$14 T for different temperatures, and (anti)symmetrized as before (the gate sweep is performed over a wider range than that in Fig. 2, therefore revealing more quantum Hall states). We observe an increase in V_{Dirac} to 2.4 V and the QHE residual longitudinal resistance R_{xx} to ≈ 600 Ω (≈ 750 Ω) for holes (electrons) at 1.7 K, indicates an increase of hole doping (and possibly disorder) from exposure to the atmosphere. A charge-neutral passivation layer similar to those reported for graphene on SiC[24] may be employed in future to preserve the graphene

quality in ambient environment. In any case, as shown in Fig. 3(a), the $i = \pm 2$ quantum Hall plateaus are still pronounced up to 60 K, showing the great potential as a quantum Hall resistance standard that can be used at much higher temperatures than those using GaAs heterostructures.

We have also characterized the zero magnetic field temperature dependent R_{xx} for this device at different ΔV_g relative to the Dirac point as shown in Fig. 3 (b), where $\Delta V_g = V_g - V_{Dirac}$, to get a qualitative indication of the disorder in the graphene. The resistance at the Dirac point increased by about 30 % with decreasing temperature between 300 K and 1.7 K. For diffusive transport in the "dirty limit", this temperature dependence is dominated by activation across potential barriers in inhomogeneous puddles.[25] The rapid increase of resistance at temperatures less than 20 K is due to the weak localization. The temperature dependence becomes non-monotonic near $\Delta V_g \approx 4$ V where the carrier density $n_s = 2.9 \times 10^{11}$ cm^{-2}, similar to results reported in Ref. [26], showing that there still exist a fair amount of impurity scattering compared with exfoliated graphene or clean CVD graphene of very small size. At the high carrier density limit ($\Delta V_g = 50$ V) where the puddle effect is suppressed, $R_{xx}(T)$ exhibits metallic behavior, indicating scattering dominated by surface phonons. A better transfer technique is desired to best preserve the quality of as-grown CVD graphene .

In summary, we have studied the magneto-transport of large scale mono layer graphene grown by CVD on Cu, then transferred to SiO$_2$/Si. In a 7 mm $\times$ 7 mm Van der Pauw geometry, these devices show half integer QHE at temperatures up to 110 K at B=14 T, with a carrier mobility near 4000 cm^2/Vs. Such CVD graphene brings promising opportunities for graphene based integrated circuits, transparent electronics, quantum Hall resistance metrology, as well as optical and STM studies due to its exceptional electronic properties kept even at very large scale.

Acknowledgments

[1] A. K. Geim and K. S. Novoselov, Nature Materials **6**, 183 (2007).

[2] Y. B. Zhang, Y. W. Tan, H. L. Stormer, and P. Kim, Nature **438**, 201 (2005).

[3] K. S. Novoselov, A. K. Geim, S. V. Morozov, D. Jiang, M. I. Katsnelson, I. V. Grigorieva, S. V. Dubonos, and A. A. Firsov, Nature **438**, 197 (2005).

[4] K. S. Novoselov, Z. Jiang, Y. Zhang, S. V. Morozov, H. L. Stormer, U. Zeitler, J. C. Maan, G. S. Boebinger, P. Kim, and A. K. Geim, Science **315**, 1379 (2007).

[5] A. J. M. Giesbers, G. Rietveld, E. Houtzager, U. Zeitler, R. Yang, K. S. Novoselov, A. K. Geim, and J. C. Maan, Applied Physics Letters **93**, 222109 (2008).

[6] A. Tzalenchuk, S. Lara-Avila, A. Kalaboukhov, S. Paolillo, M. Syvajarvi, R. Yakimova, O. Kazakova, J. J. B. M., V. Fal'ko, and S. Kubatkin, Nature Nanotechnology **5**, 186 (2010).

[7] K. S. Novoselov, A. K. Geim, S. V. Morozov, D. Jiang, Y. Zhang, S. V. Dubonos, I. V. Grigorieva, and A. A. Firsov, Science **306**, 666 (2004).

[8] T. Shen, J. J. Gu, M. Xu, Y. Q. Wu, M. L. Bolen, M. A. Capano, L. W. Engel, and P. D. Ye, Applied Physics Letters **95**, 172105 (2009).

[9] J. Jobst, D. Waldmann, F. Speck, R. Hirner, D. K. Maude, T. Seyller, and H. B. Weber, Physical Review B **81**, 195434 (2010).

[10] X. Wu, Y. Hu, M. Ruan, N. K. Madiomanana, J. Hankinson, M. Sprinkle, C. Berger, and W. A. de Heer, Applied Physics Letters **95**, 223108 (2009).

[11] K. S. Kim, Y. Zhao, H. Jang, S. Y. Lee, J. M. Kim, K. S. Kim, J.-H. Ahn, P. Kim, J.-Y. Choi, and B. H. Hong, Nature **457**, 706 (2009).

[12] H. Cao, Q. Yu, L. A. Jauregui, J. Tian, W. Wu, Z. Liu, R. Jalilian, D. K. Benjamin, Z. Jiang, J. Bao, et al., Applied Physics Letters **96**, 122106 (2010).

[13] S. Bae, H. Kim, Y. Lee, X. Xu, J.-S. Park, Y. Zheng, J. Balakrishnan, T. Lei, H. Ri Kim, Y. I. Song, et al., Nature Nanotechnology **5**, 574 (2010).

[14] J. Martin, N. Akerman, G. Ulbricht, T. Lohmann, J. H. Smet, K. von Klitzing, and A. Yacoby, Nature Physics **4**, 144 (2008).

[15] W. Wu, Z. Liu, L. A. Jauregui, Q. Yu, R. Pillai, H. Cao, J. Bao, Y. P. Chen, and S.-S. Pei, Sensors and Actuators B: Chemical **150**, 296 (2010).

[16] S. Ryu, L. Liu, S. Berciaud, Y.-J. Yu, H. Liu, P. Kim, G. W. Flynn, and L. E. Brus, Nano Letters **10**, 4944 (2010).

[17] B. N. Taylor and T. J. Witt, Metrologia **26**, 47 (1989).

[18] A. J. M. Giesbers, U. Zeitler, L. A. Ponomarenko, R. Yang, K. S. Novoselov, A. K. Geim, and

J. C. Maan, Physical Review B **80**, 241411 (2009).

[19] M. Furlan, Physical Review B **57**, 14818 (1998).

[20] F. Delahaye, Journal of Applied Physics **73**, 7914 (1993).

[21] F. Delahaye, Metrologia **31**, 367 (1995).

[22] A. Jeffery, R. E. Elmquist, and M. E. Cage, Journal of Research of the National Institute of Standards and Technology **100** (1995).

[23] S. Russo, M. Craciun, M. Yamamoto, A. Morpurgo, and S. Tarucha, Physica E: Low-dimensional Systems and Nanostructures **42**, 677 (2010).

[24] S. Lara-Avila, K. Moth-Poulsen, R. Yakimova, T. Bjϕrnholm, V. Fal'ko, A. Tzalenchuk, and S. Kubatkin, Advanced Materials **23**, 878 (2011).

[25] S. Adam and M. D. Stiles, Physical Review B **82**, 075423 (2010).

[26] J. Heo, H. J. Chung, S.-H. Lee, H. Yang, D. H. Seo, J. K. Shin, U.-I. Chung, S. Seo, E. H. Hwang, and S. Das Sarma, Physical Review B **84**, 035421 (2011).

[27] S. Kim, J. Nah, I. Jo, D. Shahrjerdi, L. Colombo, Z. Yao, E. Tutuc, and S. K. Banerjee, Applied Physics Letters **94**, 062107 (2009).

[28] S. Adam, E. H. Hwang, V. M. Galitski, and S. Das Sarma, Proceedings of the National Academy of Sciences **104**, 18392 (2007).

[29] An empirical fitting to the field effect curve (Fig. 1) according to Kim et al. [27] is used to calculate a geometry-independent residual carrier density $n_0 = 3.7 \times 10^{11}$ cm^{-2}. From n_0 and a theoretical model on graphene transport in the diffusive region by Adam et al. [28], one can extract that the impurity concentration $n_{imp} = (1.4 \pm 0.2) \times 10^{12}$ cm^{-2} and a field effect mobility $\mu = (3600 \pm 600)$ cm^2/Vs assuming a typical distance of impurities from the graphene plane, $d = (1.0 \pm 0.2)$ nm. This gives a geometrical factor (ratio between R_{xx} and resistivity ρ_{xx}) of 4.2 ± 0.7 by comparing to the empirical fitting[27] of the field effect curve.